

Neuron, Volume 103

Supplemental Information

The Serotonergic Raphe Promote

Sleep in Zebrafish and Mice

Grigorios Oikonomou, Michael Altermatt, Rong-wei Zhang, Gerard M. Coughlin, Christin Montz, Viviana Gradinaru, and David A. Prober

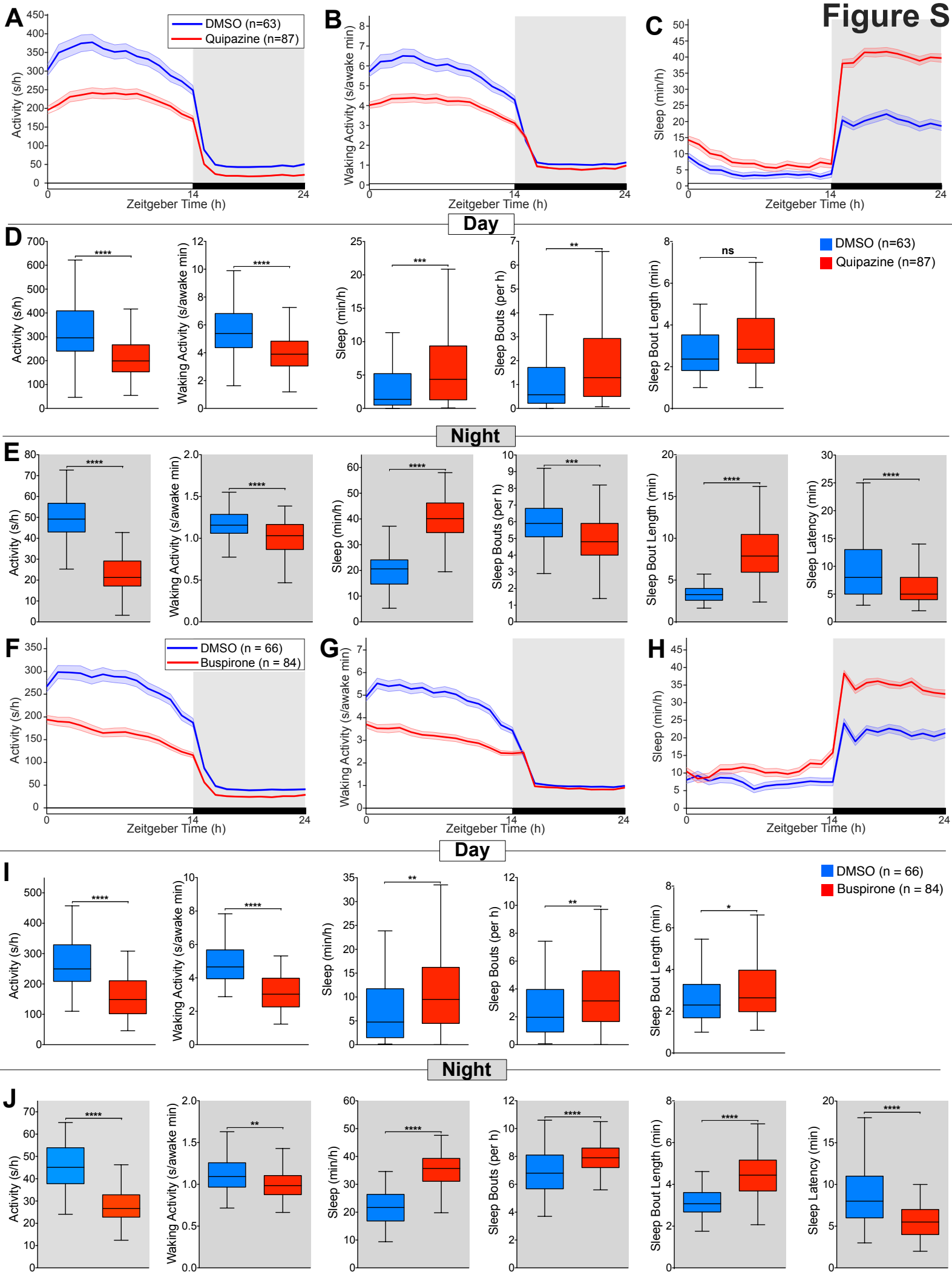


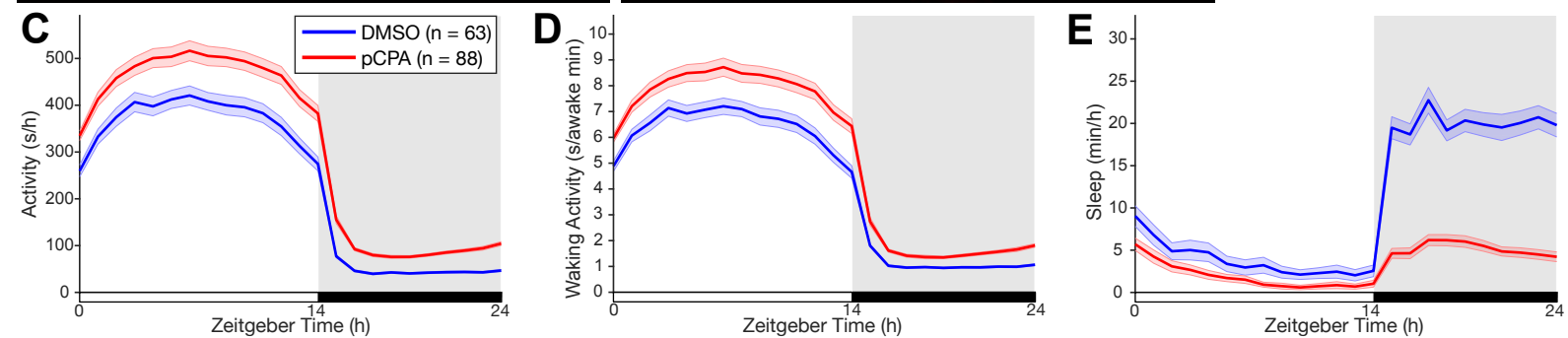
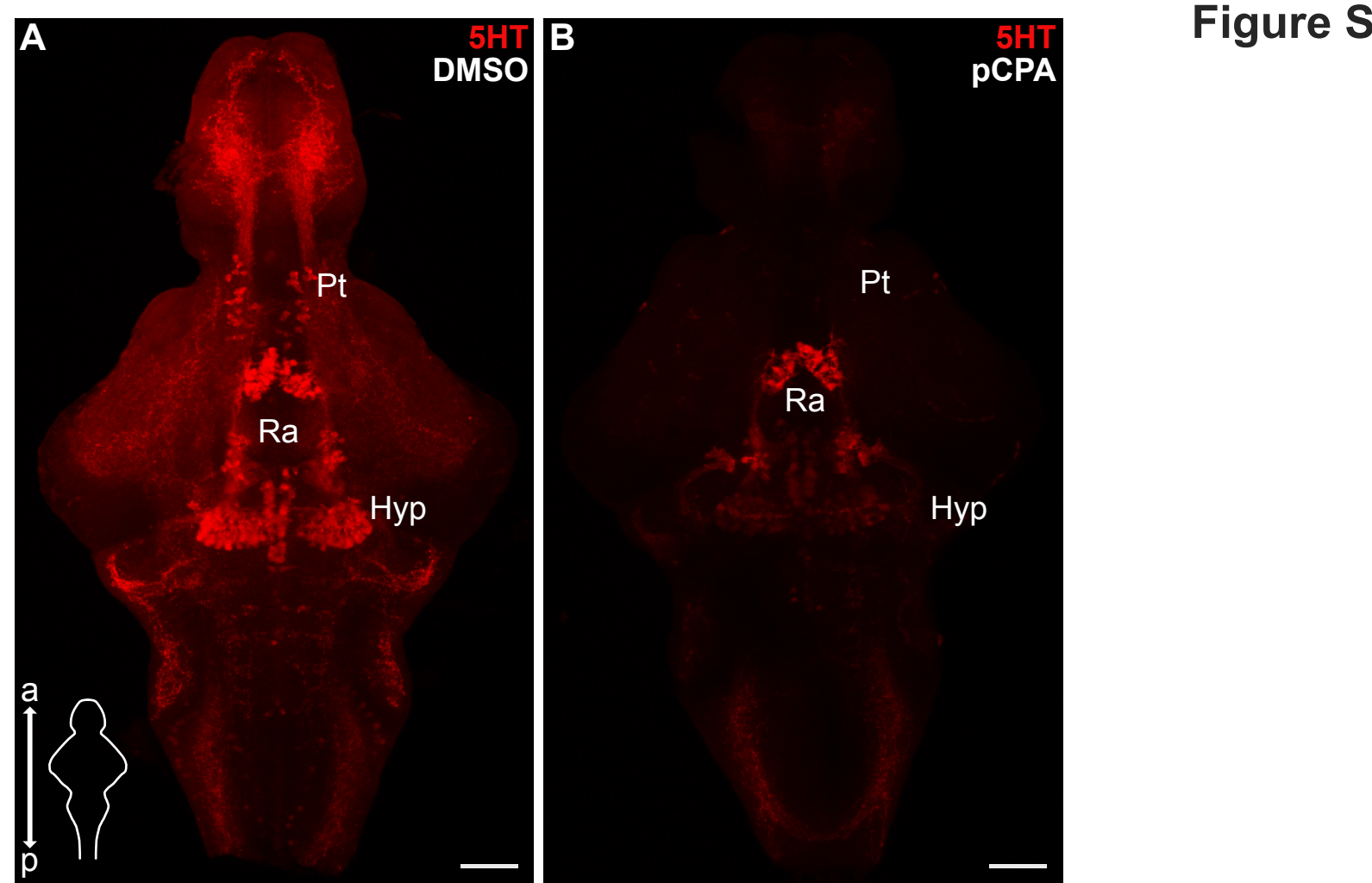
Figure S1. 5-HT receptor agonists increase zebrafish sleep, related to Figure 1.

(A-C) Activity (A), waking activity (B), and sleep (C) for zebrafish treated with DMSO vehicle (blue) or 10 μ M quipazine (red). Line and shading represent mean \pm s.e.m. n = number of animals.

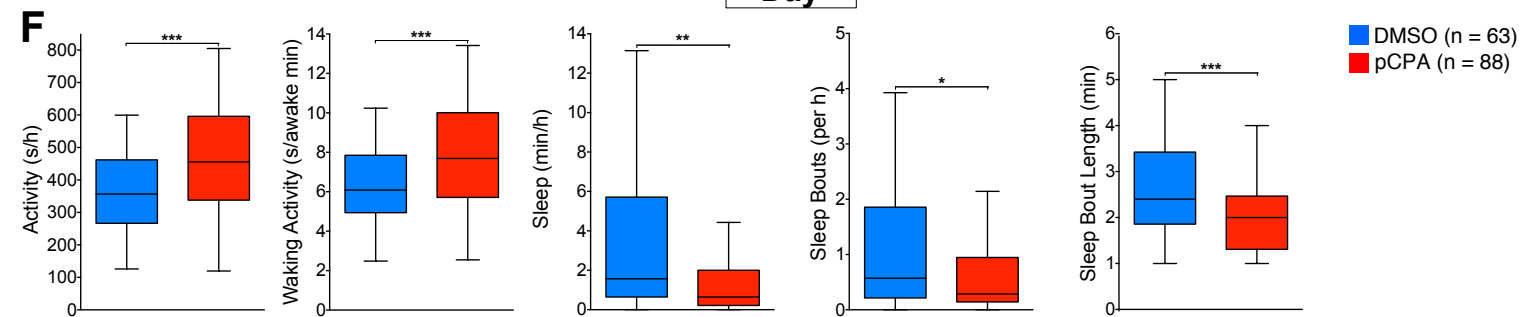
(D and E) Boxplots quantifying activity, waking activity, sleep, sleep bout number, sleep bout length during day (D) and night (E) and sleep latency during night (E).

(F-J) Same as above but for animals treated with DMSO vehicle (blue) or 25 μ M buspirone (red).

n = number of animals. ns $p > 0.05$, * $p < 0.05$, ** $p < 0.01$, *** $p < 0.001$, **** $p < 0.0001$, Mann-Whitney test.



Day



Night

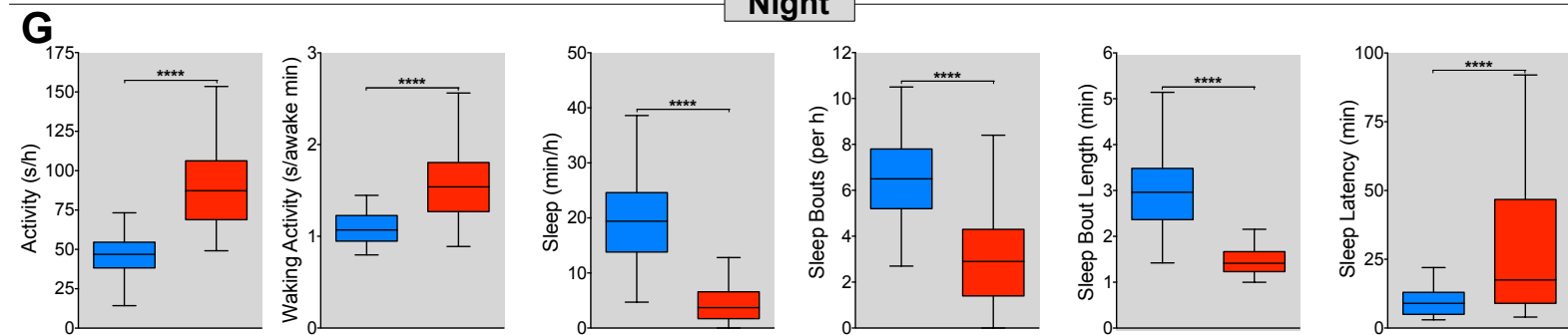


Figure S2. pCPA treatment depletes brain 5-HT and decreases sleep in zebrafish, related to Figure 1.

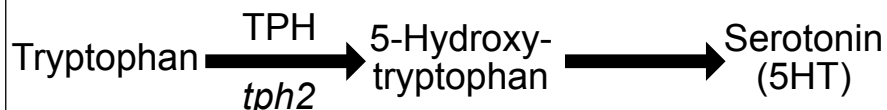
(A and B) Maximum intensity projections of dissected brains from 5 dpf zebrafish treated with either DMSO vehicle (A) or pCPA (B) and immunostained for 5-HT. Scale bar, 50 μ m; a, anterior; p, posterior; Ra, raphe; Hyp, hypothalamus; Pt, pretectal area.

(C-E) Activity (C), waking activity (D), and sleep (E) for zebrafish treated with DMSO vehicle (blue) or 7.5 μ M pCPA (red). Line and shading represent mean \pm s.e.m. n = number of animals.

(F and G) Boxplots quantifying activity, waking activity, sleep, sleep bout number, sleep bout length during day (F) and night (G) and sleep latency during night (G). n = number of animals. ns $p > 0.05$, * $p < 0.05$, ** $p < 0.01$, *** $p < 0.001$, **** $p < 0.0001$, Mann-Whitney test.

A

Raphe



Pineal gland

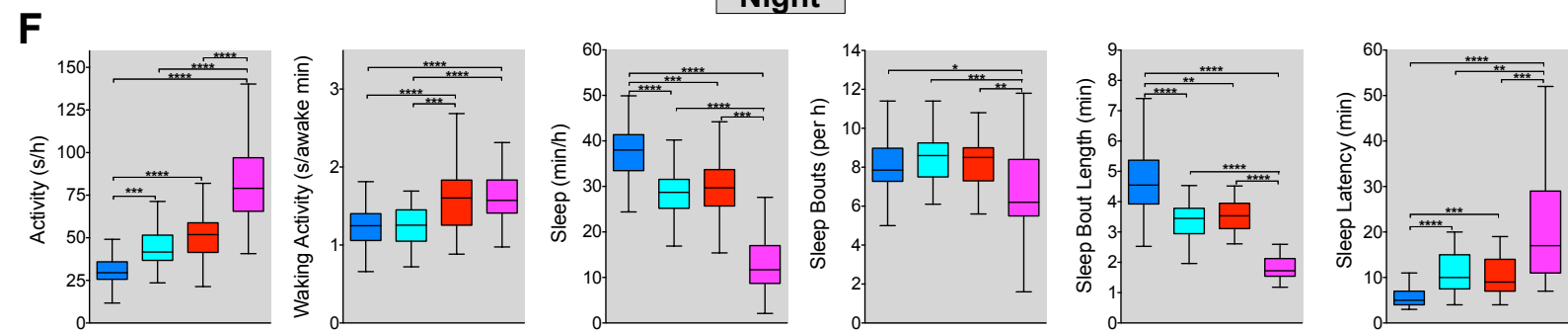
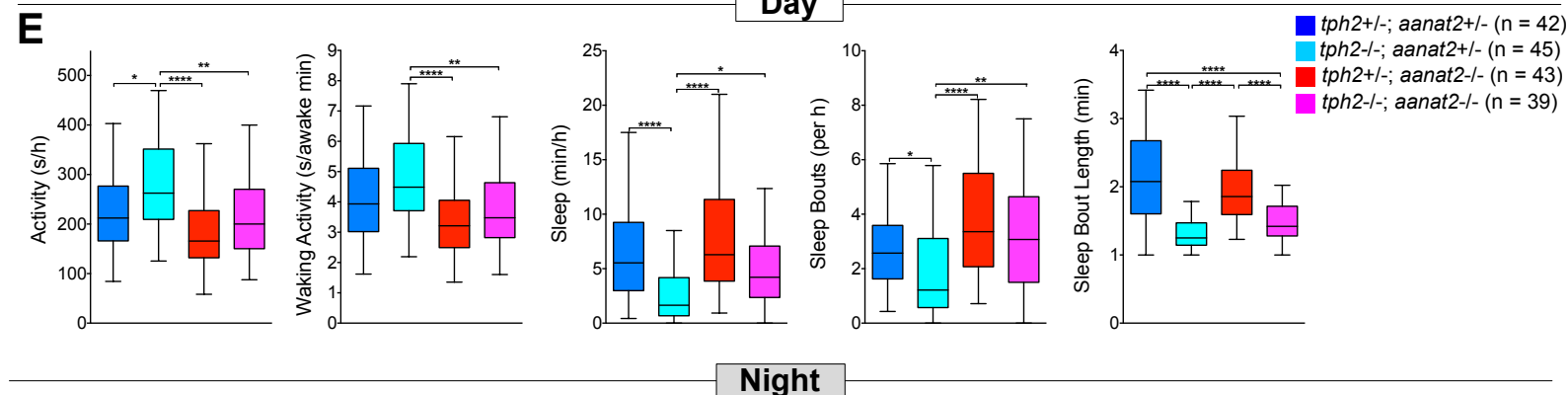
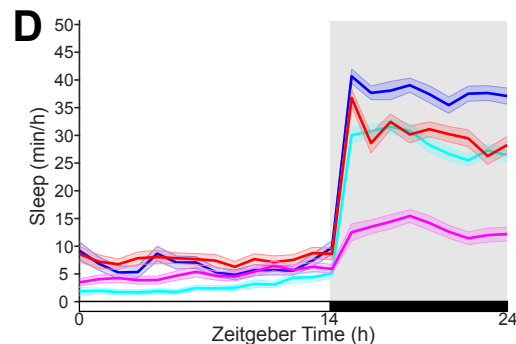
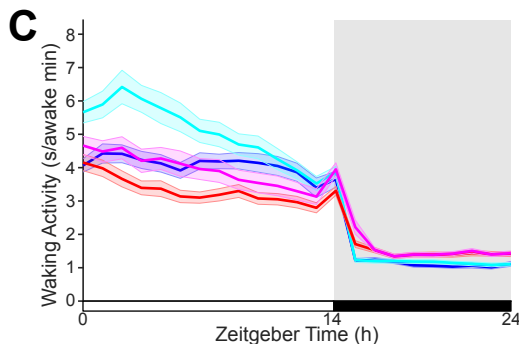
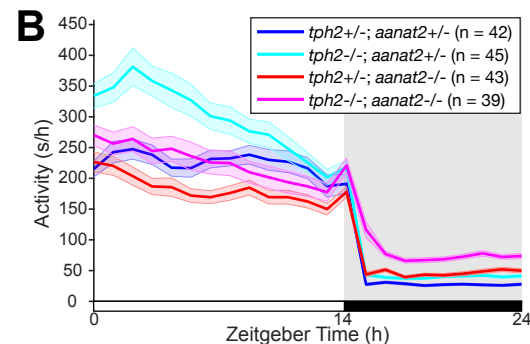
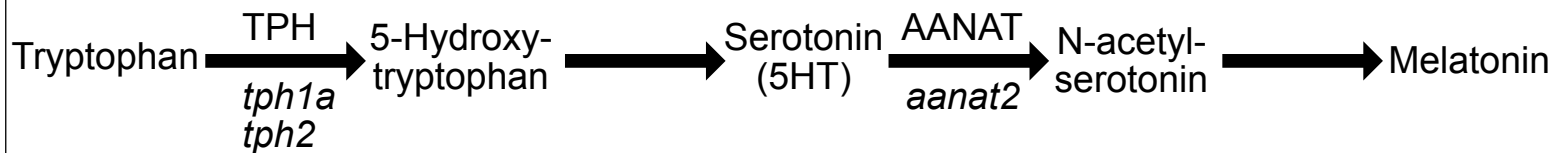


Figure S3. Loss of melatonin enhances the *tph2* mutant zebrafish night sleep phenotype, related to Figure 1.

(A) Schematic of the serotonin biosynthetic pathway in the raphe (top) where the TPH enzymatic activity originates exclusively from transcription of the *tph2* paralog, and the melatonin biosynthetic pathway in the pineal gland (bottom) where the TPH enzymatic activity originates from both *tph1a* and *tph2*. *aanat2* is expressed in the pineal and encodes for arylalkylamine N-acetyltransferase (AANAT).

(B-D) Activity (B), waking activity (C), and sleep (D) for *tph2*^{+/-}; *aanat2*^{+/-} (blue), *tph2*^{-/-}; *aanat2*^{+/-} (cyan), *tph2*^{+/-}; *aanat2*^{-/-} (red), and *tph2*^{-/-}; *aanat2*^{-/-} (magenta) zebrafish. Line and shading represent mean \pm s.e.m. n = number of animals.

(E and F) Boxplots quantifying activity, waking activity, sleep, sleep bout number, sleep bout length during day (E) and night (F) and sleep latency at night (F). n = number of animals. *p<0.05, **p<0.01, ***p<0.001, ****p<0.0001, Kruskal-Wallis test followed by Dunn's multiple comparisons test. All pair-wise comparisons were performed; only those with significant differences are indicated.

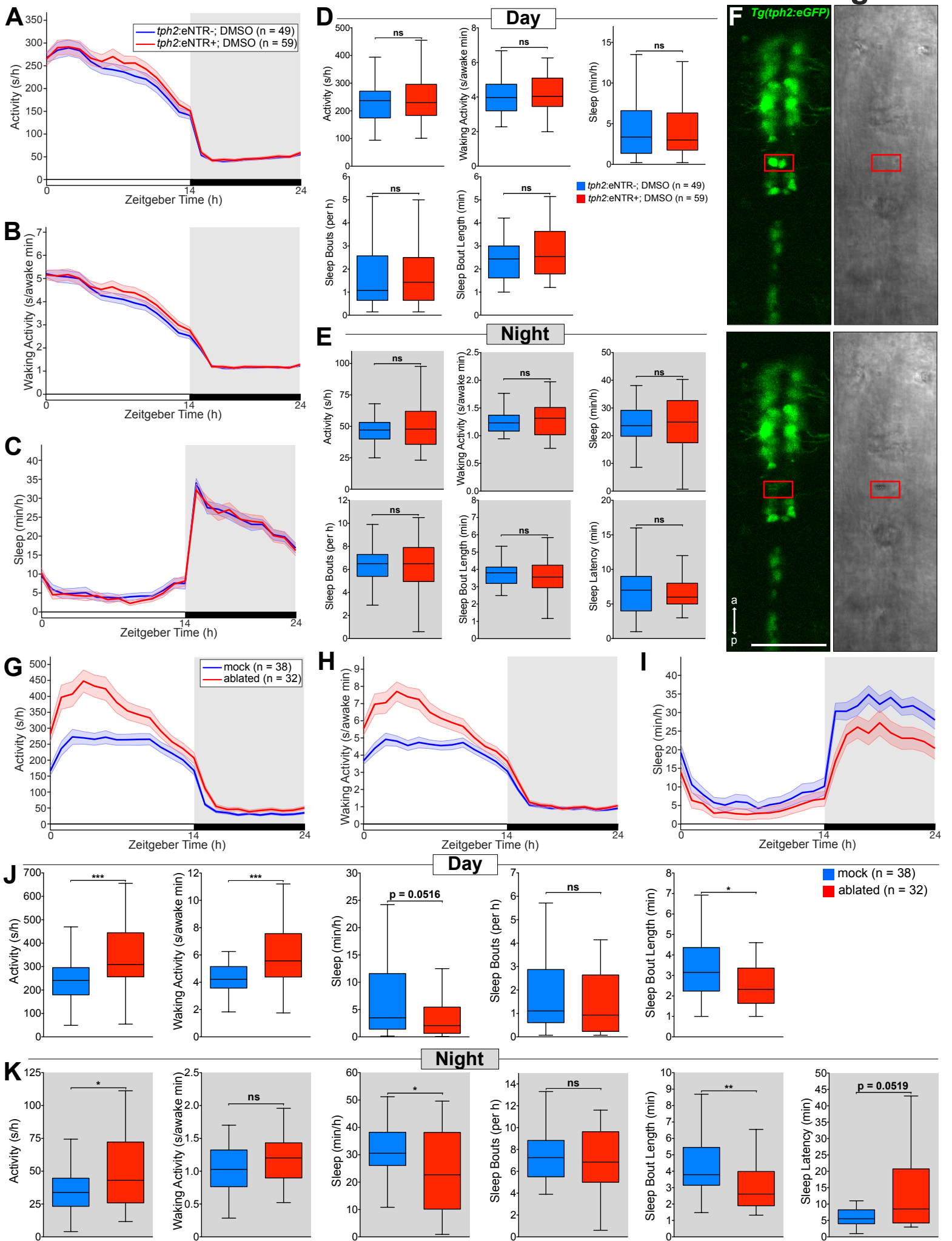


Figure S4. Vehicle treatment of *Tg(tph2:eNTR-YFP)* animals does not affect behavior; 2-photon laser ablation of the raphe results in increased locomotor activity and decreased sleep in zebrafish, related to Figure 3.

(A-C) Activity (A), waking activity (B), and sleep (C) for *Tg(tph2:eNTR-YFP)* (red) and non-transgenic sibling control (blue) zebrafish treated with DMSO. Line and shading represent mean \pm s.e.m.

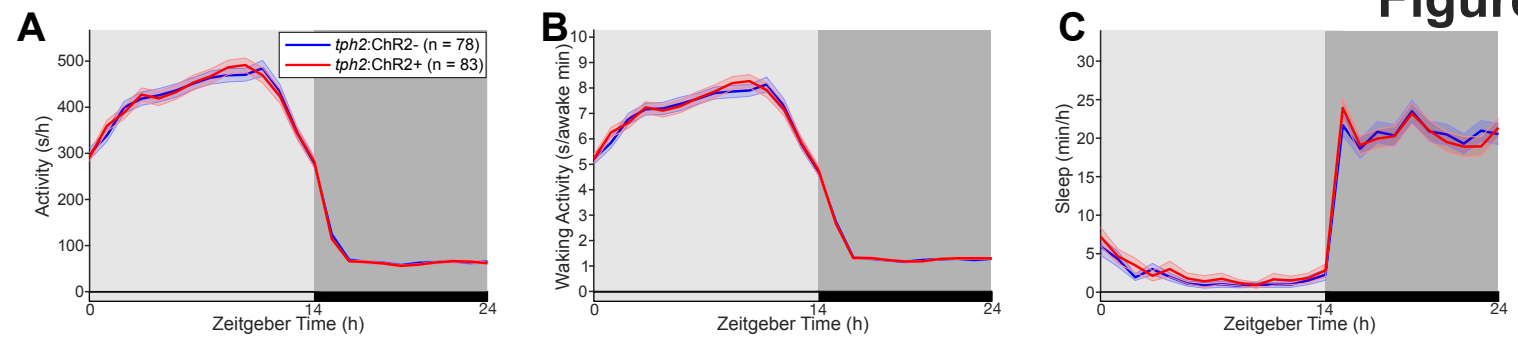
(D and E) Boxplots quantifying activity, waking activity, sleep, sleep bout number, sleep bout length during day (D) and night (E) and sleep latency during night (E).

(F) Top: Image of *Tg(tph2:eGFP)* fish (green channel on left, transmitted light image on right) before ablation of cells in red box. Bottom: Same as above but after 2-photon laser ablation; note small cavitation in transmitted light image (red box). The same process was repeated until all GFP+ cells in the shown area were ablated. Scale bar, 50 μ m; a, anterior; p, posterior.

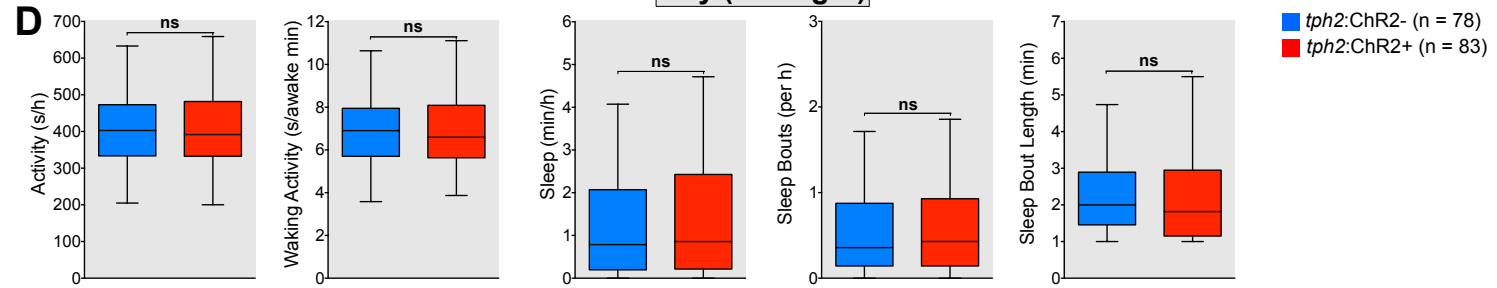
(G-I) Activity (G), waking activity (H), and sleep (I) for raphe laser-ablated (red) and mock laser-ablated sibling control (blue) zebrafish. Line and shading represent mean \pm s.e.m.

(J and K) Boxplots quantifying activity, waking activity, sleep, sleep bout number, sleep bout length during day (J) and night (K) and sleep latency during night (K).

n = number of animals. ns $p > 0.05$, * $p < 0.05$, ** $p < 0.01$, *** $p < 0.001$, Mann-Whitney test.



Day (dim light)



Night

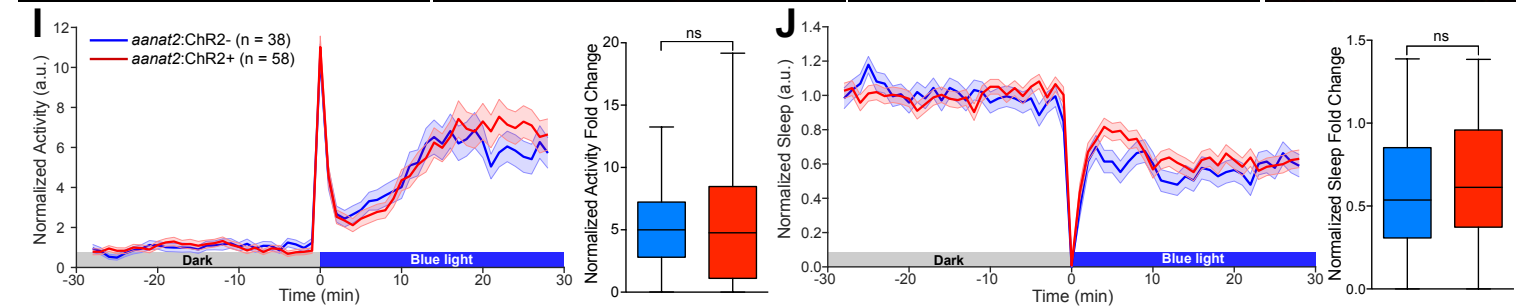
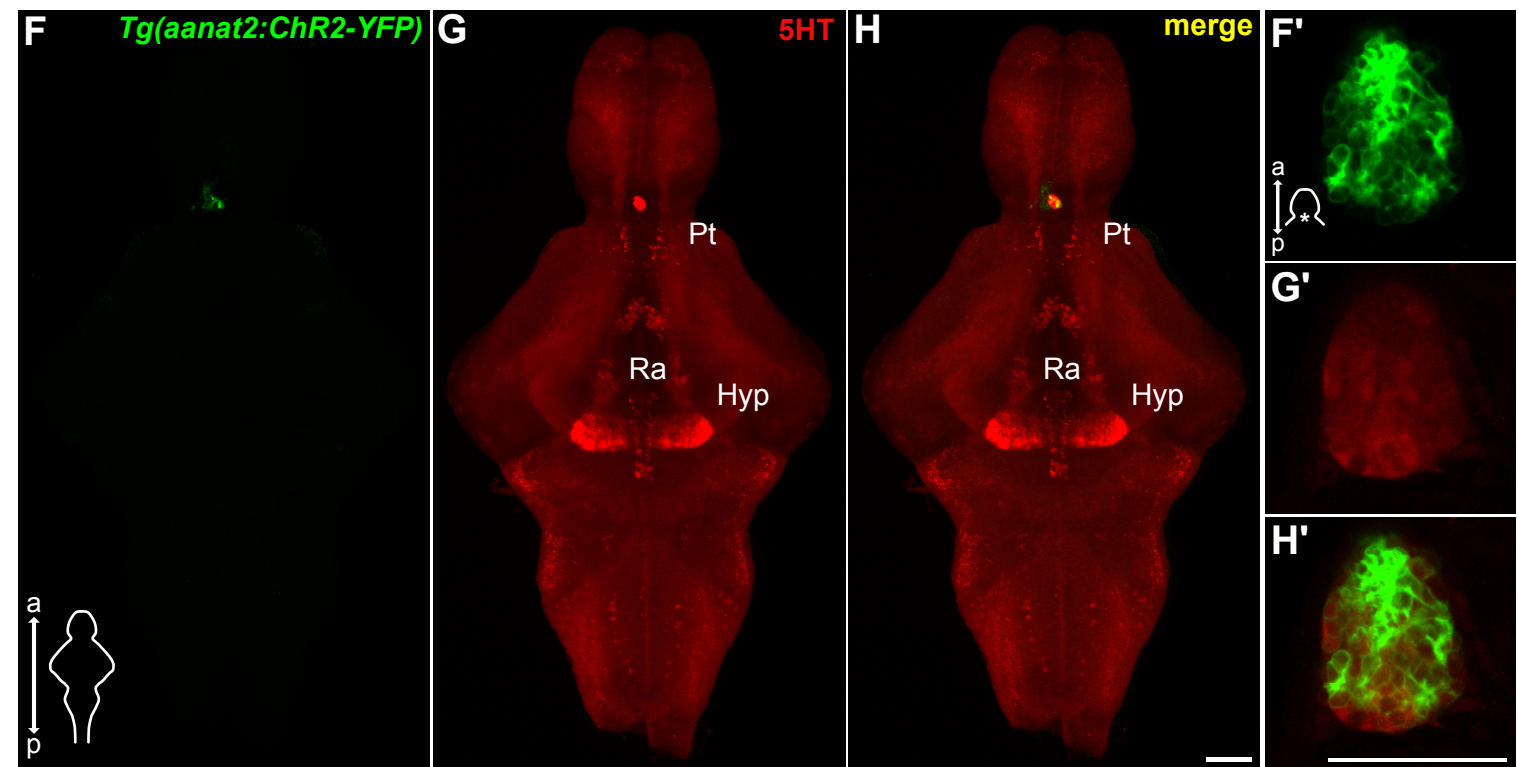
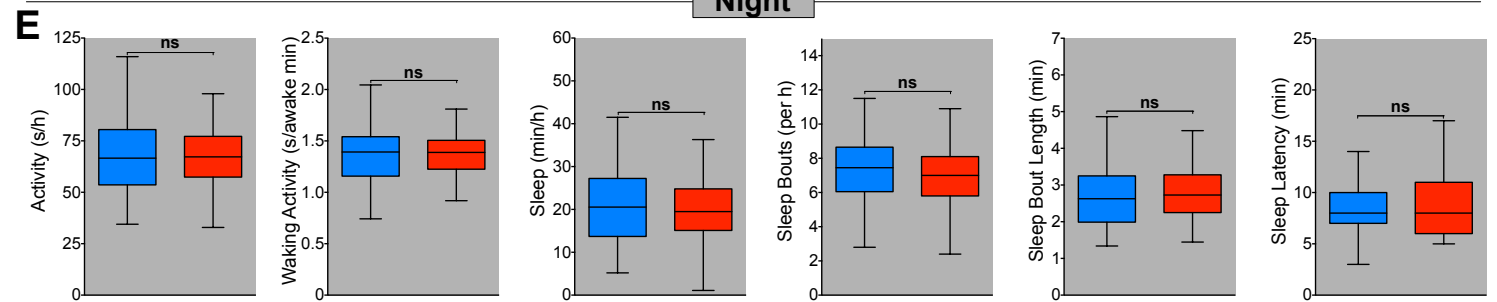


Figure S5. *Tg(tph2:ChR2-YFP)* zebrafish show normal wake/sleep cycles when maintained in dim light/dark cycles; blue light exposure does not affect behavior in zebrafish that express ChR2 in the pineal gland, related to Figure 4.

(A-C) Activity (A), waking activity (B), and sleep (C) for *Tg(tph2:ChR2-eGFP)* (red) and non-transgenic sibling control (blue) zebrafish maintained in a dim light/dark cycle. Line and shading represent mean \pm s.e.m. n = number of animals.

(D and E) Boxplots quantifying activity, waking activity, sleep, sleep bout number, sleep bout length during day (D) and night (E) and sleep latency during night (E). n = number of animals. ns $p > 0.05$, Mann-Whitney test.

(F-H') Maximum intensity projections of dissected brains from 5 dpf *Tg(aanat2:ChR2-YFP)* zebrafish immunostained for 5-HT and YFP. a, anterior; p, posterior; Pt, pretectal area; Hyp, hypothalamus; Ra, raphe. The 5-HT+ structure above the Pt is the remnants of the pineal gland that was damaged during dissection. (F'-H') Single plane images of the pineal gland from 5 dpf *Tg(aanat2:ChR2-YFP)* whole zebrafish immunostained for 5-HT and YFP. Scale bars, 50 μ m.

(I, J) Left: Normalized locomotor activity (I) and sleep (J) traces of 5 dpf *Tg(aanat2:ChR2)* zebrafish (red) and non-transgenic siblings (blue) before and during exposure to blue light. Right: boxplots quantifying normalized locomotor activity (I) and sleep (J) fold change during illumination. Line and shading represent mean \pm s.e.m. n = number of animals; 3 trials per animal. ns $p > 0.05$, Mann-Whitney test.

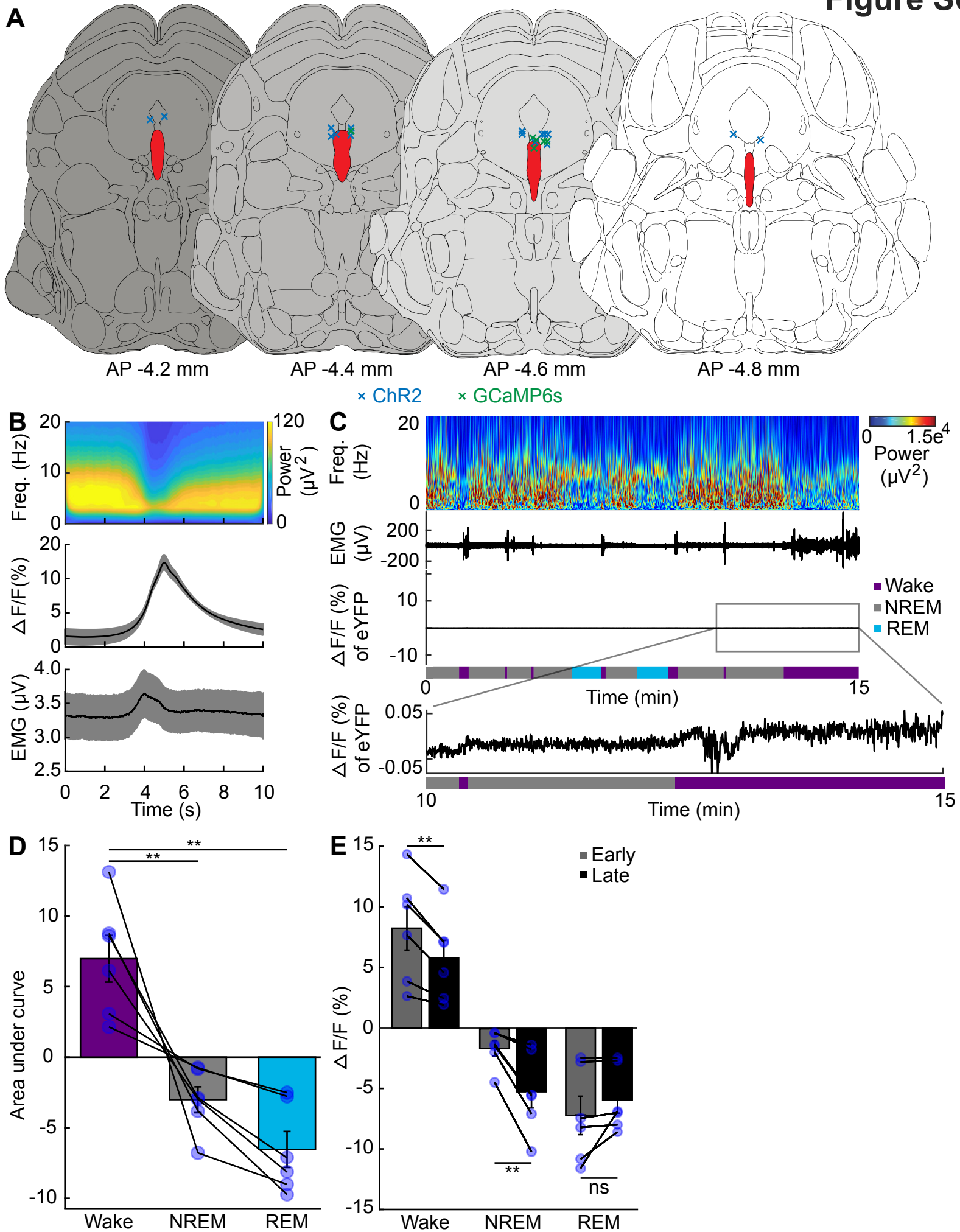


Figure S6. Large fluorescence changes of DRN^{SERT-GCaMP6s}, but not DRN^{SERT-eYFP}, across and within behavioral states, related to Figure 5.

(A) Fiber-tip locations of DRN^{SERT-ChR2} (blue) and DRN^{SERT-GCaMP6s} (green) mice.

(B) EMG signal and spectral analysis of EEG traces around fluorescent peaks from DRN^{SERT-GCaMP6s} during NREM episodes.

(C) Representative example from a DRN^{SERT-eYFP} mouse of spectrogram, EMG and fiber photometry traces over time across different sleep-wake states. Last 5 min of $\Delta F/F$ (%) of eYFP are magnified to illustrate minor locomotion-induced artifacts.

(D) Activity level of DRN^{SERT} averaged across normalized time per state (one-way ANOVA followed by Bonferroni post hoc test).

(E) Comparison of DRN^{SERT} activity levels early and late (10-20 and 80-90 percentile time ranges, respectively) within episodes of wake, NREM and REM states (paired t test).

n = 6 DRN^{SERT-GCaMP6s} mice; ns p>0.05, **p< 0.01. Data represent mean \pm sem.

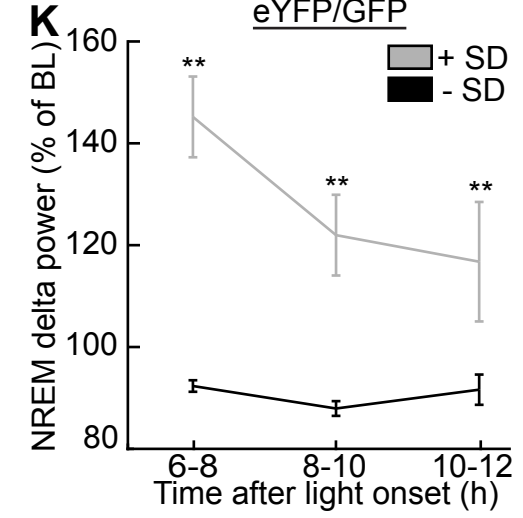
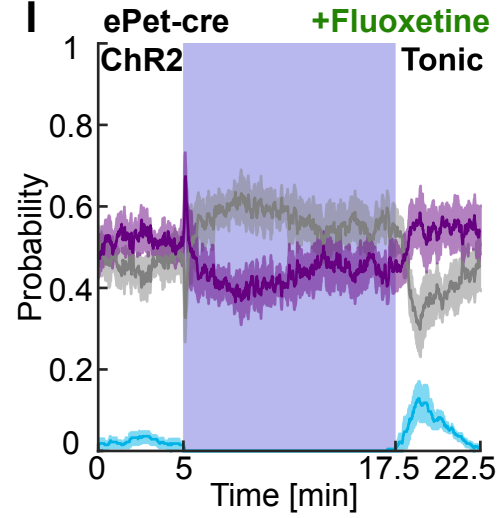
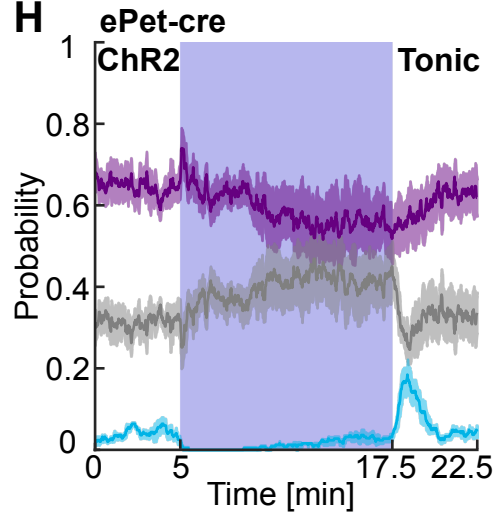
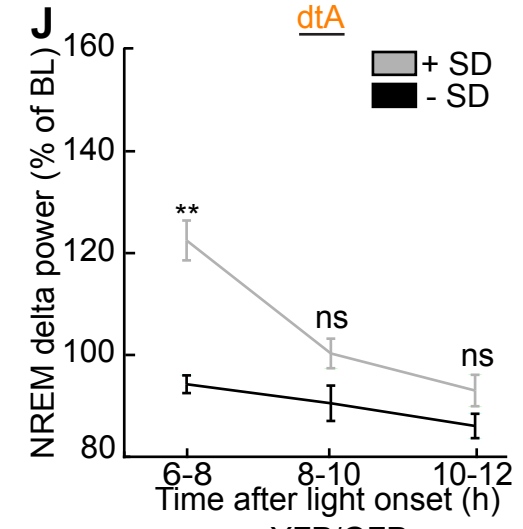
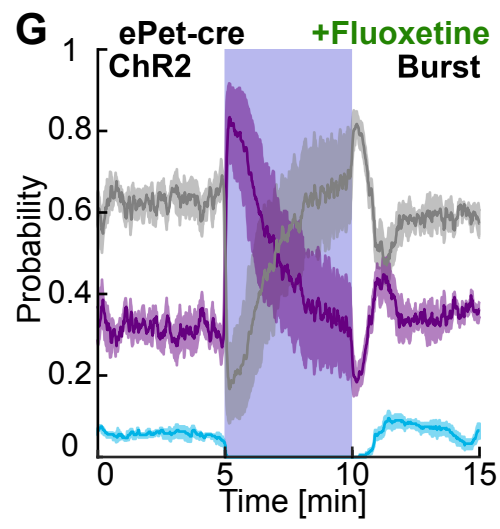
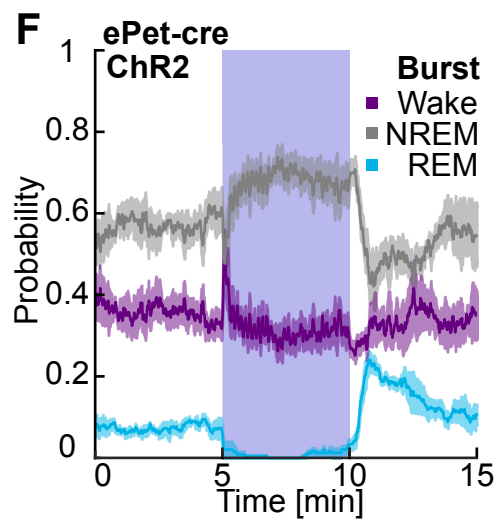
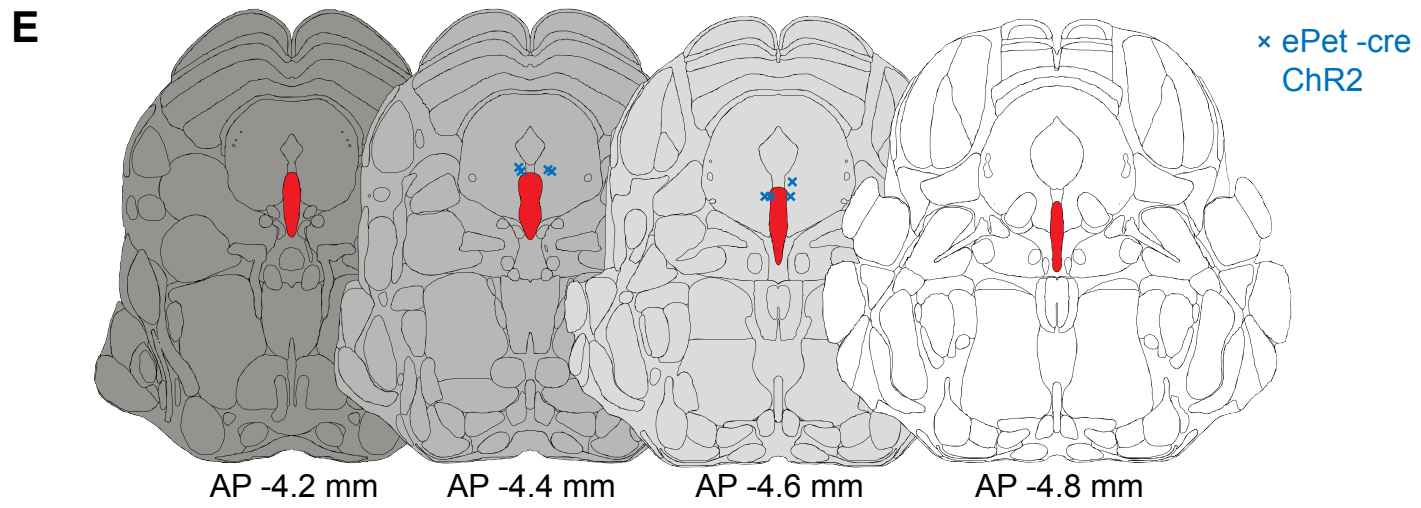
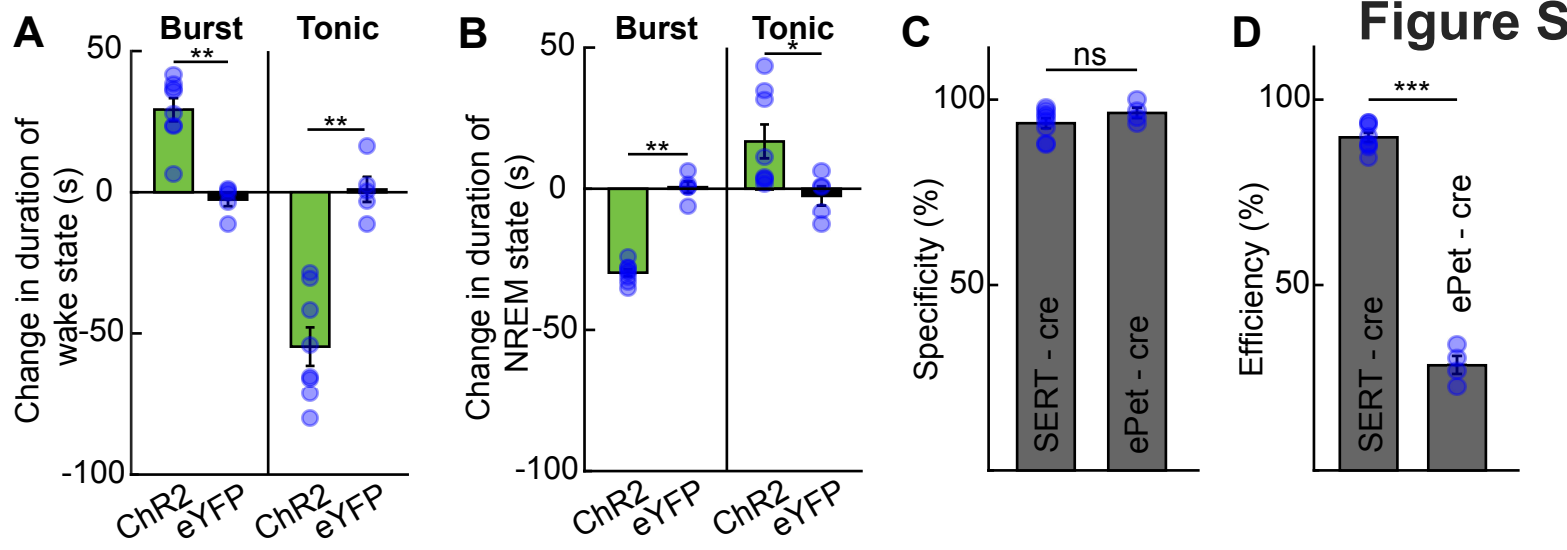


Figure S7. Optogenetic stimulation of DRN using different transgenic mouse lines; change in delta power after SD of B5-B9^{SERT-dtA} and B5-B9^{SERT-eYFP} or B5-B9^{GFP} mice, related to Figures 6 and 7.

(A) Change in duration of wake state during burst or tonic stimulation of DRN^{SERT-ChR2} and DRN^{SERT-eYFP} mice (n = 8 for DRN^{SERT-ChR2}; n = 5 for DRN^{SERT-eYFP}; two-sided Wilcoxon rank sum test, **p<0.01).

(B) Change in duration of NREM state during burst or tonic stimulation of DRN^{SERT-ChR2} and DRN^{SERT-eYFP} mice (n = 8 for DRN^{SERT-ChR2}, n = 5 for DRN^{SERT-eYFP} two-sided Wilcoxon rank sum test, **p<0.01, *p<0.05).

(C-D) Quantification of viral transduction efficiency ((ChR2+ & TPH2+)/TPH2+) and ChR2-eYFP expression specificity ((ChR2+ & TPH2+)/ChR2+) in SERT-cre (Zhuang et al., 2005) and ePet-cre (Scott et al., 2005) mice (n = 8 for DRN^{SERT-ChR2}, n = 4 for DRN^{ePet-ChR2}, paired t test, ns p>0.05, ***p<0.001).

(E) Fiber-tip locations of ePet-cre (Scott et al., 2005) mice injected with AAV5-EF1a-DIO-ChR2-eYFP (n = 4 for DRN^{ePet-ChR2}).

(F) Burst stimulation of DRN^{ePet-ChR2} neurons. Blue box highlights laser stimulation period (n = 4 DRN^{ePet-ChR2}).

(G) Same experiment as (F), but with prior i.p. injection of 10-20 mg/kg fluoxetine (n = 4 DRN^{ePet-ChR2}).

(H) Tonic stimulation of DRN^{ePet-ChR2} neurons (n = 4 DRN^{ePet-ChR2}).

(I) Same experiment as (H), but with prior i.p. injection of 10-20 mg/kg fluoxetine (n = 4 DRN^{ePet-ChR2}).

(J) Delta power in NREM episodes across the last 6 h of the light phase with and without prior 6 h SD of B5-B9^{SERT-dtA}. Delta power is shown as percentage of average delta power across all NREM episodes during the light phase (n = 8 for B5-B9^{SERT-dtA}, two-sided Wilcoxon signed rank test, ns p>0.05, **p<0.01).

(K) Delta power in NREM episodes across the last 6 h of the light phase with and without prior 6 h SD of B5-B9^{SERT-eYFP} or B5-B9^{GFP}. Delta power is shown as percentage of average delta power across all NREM episodes during the light phase (n = 8 for B5-B9^{SERT-eYFP} or B5-B9^{GFP}, two-sided Wilcoxon signed rank test, **p<0.01). Data represent mean ± sem.